Proc. of SPIE Vol. 1739, High Heat Flux Engineering, ed. A M Khounsary (Feb 1993) Copyright SPIE

Design of a high pressure/high thermal flux window lens of low polarization and phase distortion

James L. Reeve and Andrew G. McKay

TRW Space and Defense Sector, Optical and Mechanical Products Department
One Space Park, Redondo Beach, CA, 90278

ABSTRACT

Flat transmissive material windows are often used in high power CW laser systems to separate a low pressure resonator cavity from a one atmosphere beam train. Recently a requirement was identified for a pressure cell window that would transmit intensity peaks of 31 KW/cm2 for 5 seconds, react a differential pressure of 52 ATM without active cooling, and focus the incident light as a lens. Budgeted optical distortion levels were 400 nm of rms wave front error and no more than 0.01 % conversion of s polarization state into p state through window birefringence. The design of this window is described, including material selection, thermal and structural finite element analysis, Wiebull strength evaluation, measurement and selection of single crystal blanks with low internal stress, evaluation of phase and polarization distortion and mounting considerations.

2. INTRODUCTION

A unique requirement for an optical window arose as a key part of the design of a high pressure gas cell for phase conjugation experiments at HF laser wavelength. The window is mounted in a side port of a pressure vessel containing inert gas at 52 to 55 atmospheres pressure. Figure 1 shows the essential cell geometry. A collimated laser beam is directed at the window from the left and is brought to focus within the gas volume by the window acting as a thick lens. The laser intensity at focus exceeds the threshold necessary to initiate a stimulated Brillouin scattering (SBS) process. Up to 80 percent of the input power is reflected from the SBS grating, passing back out the input window. This phase conjugate of the input pump beam. The remaining transmitted power exits the cell through a similar window/lens.

Thus the input window of the gas cell must withstand about 1.8 times the intensity of the input laser beam while reacting the experiment gas pressure of 55 atmosphere maximum. The similar rear window need only withstand the 20% intensity of the transmitted beam with good optical performance, although it must be capable of transmitting the full power of the laser beam in case the SBS phenomenon were to fail to start.

While the phase conjugation process is intended to correct for large phase errors in the input beam, it is desired to perform the experiment with a fairly high quality beam, both for ease of diagnostic interpretation and for the fact that wave front errors decrease the intensity at the SBS cell focus, thus raising the power threshold that must be exceeded. Hence a minimum input window wave front error was desired.

The phase conjugate reflected beam is coaligned with the input beam, but is prevented from returning to the laser resonator by an isolation system. The isolation system discriminates between the incident and return beams by their orthogonal polarization states and directs the returning beam away from the resonator into a calorimeter and other diagnostics. Isolation by polarization imposes stringent limits on the birefringence of most of the optics in the train including the SBS cell input window. Any birefringence shift of power from s to p polarization will result in reflected power leaking back into the laser resonator. Feedback into the laser will degrade output beam quality and high values can damage resonator mirrors.

Cost and schedule considerations motivated a desire to grind these thick lens windows from existing flat window blanks. This constraint set the maximum thickness and diameter of the window. These requirements are summarized in Table 1, along with the predicted performance of the design.

3. DESIGN ANALYSIS

3.1 Material Selection and Preliminary Design

Leading window materials at IR wavelengths were surveyed to find which offered the best combination of properties for a heat sink cooled pressure window. Classical methods [1,2] for round constant thickness plates under pressure load and one dimensional slabs under thermal load were used to find conservative estimates of window thickness, surface temperature rise, wave front error and birefringence. While approximate, the relative values of these quantities indicate the most favorable materials. Table 2 shows this material comparison. The best choice was <111> oriented single crystal CaF_2. Cost considerations dictated utilizing some existing flat window blanks of this material.

3.2 Finite Element Analysis

Figure 2 shows a finite element model of the window constructed in the PATRAN modeling code. The PTHERMAL section of that code was used to apply volumetric and surface heating proportional to the spatially varying intensity within the beam footprint and predict transient temperatures for 1 to 5 seconds exposure. Load cases representing gas pressure, beam heating and sealing preload were constructed and evaluated using NASTRAN as the structural solver. The stress and deflection result files were then passed back to PATRAN for post processing and plotting. Note that the slightly off center beam footprint on the window is modeled with an evenly spaced rectangular grid. Transition to the cylindrical coordinates of the lens and its support is made outside the heated zone. This strategy reduces the complexity of interpolation on both input and output.

Plots exaggerating the deformation patterns of the separate load cases are shown in figures 3, 4 and 5. The stress levels that occur in the window from superpositions of these load cases, i.e. seal preload, seal preload plus pressure and preload plus pressure plus beam heating were then examined to determine the structural integrity of the window.

3.3 Window Reliability Determination

Single crystal calcium fluoride is a relatively soft, brittle material. Its tensile strength is highly sensitive to surface defects and the area exposed to any given surface tensile stress. Tensile stresses in the interior of the window, away from surface defects are of lesser importance for failure prediction. The material can also slip under shear stress along certain crystallographic planes. Failure under slow crack growth has not been observed. The reliability of the window was evaluated with a Weibull probability integral per Iden and Detrio[3]:

$$\ln(1-F) = \int_A [(\frac{\sigma_1}{\sigma_0})^\gamma + (\frac{\sigma_2}{\sigma_2})^\gamma] dA \qquad (1)$$

where a value of F, the probability of window failure, of less than 5% was considered acceptable. In equation (1) σ is principle tensile stress at the window surface in each of two orthogonal directions and A is surface area. The Weibull scale and shape parameters, σ_o and γ, were taken to be 8500 $lb_f\text{-}in^{-1.327}$ and 2.97 respectively for CaF_2.

Table 3 shows the results of this process. The highest probability of failure occurs with the window pressurized without being preloaded into its mount, which would not normally occur. The next highest probability occurs with preload plus pressure. Adding beam heating tends to superimpose compression over an area around the center of the window which is under high tension from pressurization.

3.4 Wave Front Error and Birefringence Evaluation

The window's optical path difference(OPD) from its unstressed, isothermal state was found from:

$$OPD(i) = (n-1)(\delta_{z,front} - \delta_{z,rear}) + \int_{ray\ i} [\frac{\partial n}{\partial T} \Delta T] dz \qquad (2)$$

where z is a coordinate parallel to the laser beam, n = index of refraction, δ = displacement and ΔT = temperature rise. This integral was evaluated for 289 equally spaced rays through the window and the results rms averaged. A phase distortion of 0.039 rms HF waves was found about a 0.028 HF wave piston component after 5 seconds of irradiation.

Similarly the birefringence induced in the window by service conditions was calculated along the same rays by:

$$B(i) = \int_{ray\ i} [\frac{n^3(q_{11}-q_{22})(\sigma_1-\sigma_2)}{2\lambda}] dz \qquad (3)$$

where B(i) = retardation along ray i and q11 and q_{22} are piezoptic constants. Equation (3) actually predicts retardation with the <100> direction parallel to the light. Joiner et al [5] found that the result of equation (3) can be multiplied by a factor $q_{66}/(q_{11}-q_{22})$, which is much less than unity when light traverses the CaF_2

lattice nearly normal to the <111> plane. As our window blanks had been specified <111> oriented, we anticipated some reduction in the rms value of B, but no confirming data were available.

Further, use of equation(3) can predict birefringence from known pressure and thermal stresses. Any single crystal window blank will show initial birefringence due to internal stresses that must be combined with that produced by the service conditions. This internal stress birefringence is a function of crystal orientation, the location and angle that the blank was cut from the boule and the growth and annealing history of the blank. A test program was thus needed to measure local values of internal stress birefringence over each window blank and select one with low retardation within the beam footprint.

4. EXPERIMENTAL PROGRAM

The intent of the experimental program was to gather data that would allow the construction of accurate models to predict the effect of the windows on the polarization state of a transmitted wavefront. It was desired both to determine what levels of birefringence would be present in unloaded windows and what levels of birefringence would be present due to anticipated loads.

4.1 Apparatus

A survey of various retardation measurement methods was performed. Because it was desired to resolve 0.5 nm retardation the number of options was limited. It was decided to use the method of spectral contents analysis as described by Redmer[4]. A Stainoptics Technology model EO-1500-SCA instrument was acquired for this purpose.

4.2 Orientation Effects

Optimal orientations for slightly strained crystals have been discussed by Joiner[5]. A single crystal calcium fluoride window with its <111> crystal axis oriented normal to the plane of window was measured to verify the property predicted by Joiner. The window was rotated about an axis in the plane of the window surface and orthogonal to the plane of incidence. The change in retardation vs. angle of incidence is presented in figure 6. The experimental results are in general agreement with the result predicted by Joiner. The differences between the theoretical prediction and the experimental results are probably due to experimental error arises from slightly different volumes of crystal being sampled as the angle of incidence changed. Orientation effects in slightly strained calcium fluoride are a weak effect. Also since large "single" crystals are variable the optimal orientation of the window changes from location to location across the window. Because of this crystal orientation was not used to minimize the birefringence effects.

4.3 Thermal Durability and Birefringence Testing

Since the window will be heated by the laser used to initiate the SBS process the effect of thermally induced stress birefringence was studied. Previous work by Hordvik[6] indicated that absorption of incident radiation would be dominated by surface effects. The level of stress and birefringence was expected to be greater when large thermal gradients were present. In order to simulate the effect of heating the window by a high energy laser a test sample was heated by three methods. The surface of the window was heated by hot air with a generated by a heat gun, by contact with a 20 W soldering iron and by heating with a propane flame. The temperature rise was monitored by a thermocouple bonded to the surface of the test

sample. The results of this test are presented in figure 8. Temperature rises of 20° C resulted in increase retardance of 2.0 to 2.7 nm. Temperature rises in excess of 100° C resulted in <5 nm change in measured retardance. Under heating with a high energy laser the increase in phase retardation would be expect to be twice as much due to heating of two sides of the window.

4.4 Window Blank Intrinsic Birefringence

Some strain is present even in nominally unloaded crystals due to strain that is intrinsic to the crystal lattice. These strains may be due to thermal gradients that are present during the crystal growth process or due to mechanical dislocations that occur during the optical fabrication process. Also the stresses and resultant birefringences within a "single" crystal can be non-uniform possibly due to slippage's in the crystal lattice. In order to quantify the levels of intrinsic birefringence four windows, each nominally 150 mm in diameter, were mapped. Figure 9 shows a retardation map of the least birefringence window measured. A RMS average variation of 0.6 nm retardation was calculated for this blank. This was an exceptionally uniform blank. The other three windows measured had RMS birefringence variations that ranged from 2.6 to 7.0 nm.

5. CONCLUSIONS

Material windows are capable of satisfying the stringent strength, aberration and depolarization requirements of SBS gas cells for irradiation times up to at least 5 seconds. Active cooling of such windows, perhaps combined with advanced materials and coatings offering lower IR absorption levels, will allow steady state operation of such cells in many applications.

6. ACKNOWLEDGMENTS

This design effort was supported under Naval Research Laboratory Contract No. N00014-89-C-2331. Dr. B. J. Feldman and Dr. W. T. Whitney, technical monitors. The authors wish to acknowledge the contribution of D. J. Cambron to the finite element analysis.

7. REFERENCES

1. R. Roark and W. Young, Formulas for Stress and Strain, 5th Ed., Mc Graw-Hill, 1975.
2. H. Carslaw and J. Jaeger, Conduction of Heat in Solids,2 nd.Ed.,Oxford Univ. Press, 1959.
3. AFWAL-TR-83-4059, Optical Window Mechanical Strength and Reliability, by J. Iden, J. Detrio, and J. Fox, Air Force Wright Aeronautical Laboratories, June, 1983.
4. A. Redner, "Photoelastic Measurements by Means of Computer Assisted Spectral Contents Analysis",Experimental Mechanics, Vol.25, No.2, 148-153, June 1985.
5. R. Joiner, J. Marburger and W. Steier, "Critical Orientations for Eliminating Stress-Induced Depolarization in Crystalline Windows and Rods", in Laser Induced Damage in Optical Materials: 1977 (NBS-SP-509), p 89.
6. C. Klein, "Stress Induced Birefringence, Critical Window Orientation, and Thermal Lensing Experiments", Twelfth Annual Symposium on Optical Materials for High Power Lasers, NBS, September, 1980.
7. A. Hordvik and L. Skolnik, "Photoacoustic Measurements of Surface and Bulk Absorption in HF/DF laser window materials", Applied Optics, Vol 16, No. 11, Nov. 1977.

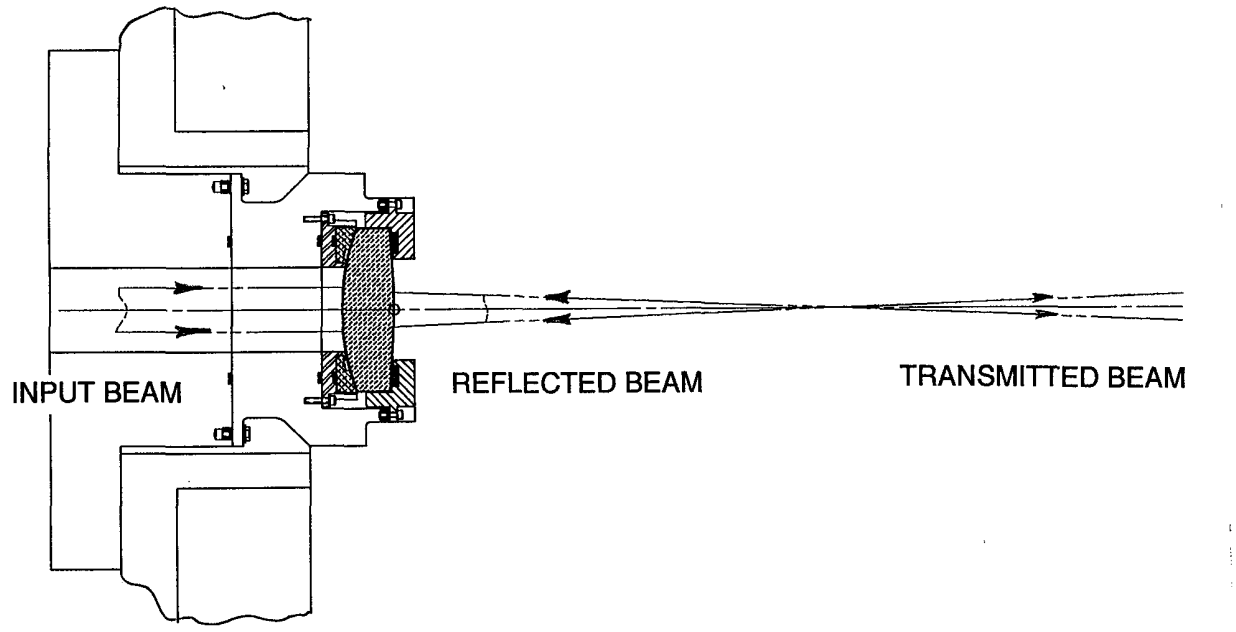

Figure 1 - SBS Cell Window Mounting

Table 1 - Window Requirements and Predicted Performance

Parameter	Requirement	Capability
Run Time	5 sec.	✔
Focal length	40 cm	✔
Wavelength	2.9 micron	✔
Pressure	55 ATM. maximum, beam on/65 ATM. max., beam off	✔
Peak Intensity	31 KW/cm2	✔
Survivability	< 5% chance of failure	<1.15%
Window Pressure Aperture	> 6.9 cm.	7.70 cm clear dia., 8.72 cm to seal
Use existing window blank	4.7 cm max. thickness 14.8 cm diameter	✔
Surface temperature rise	Coating temperature shall not exceed 100 C	30 C rise at peak 3.2 C at average intensity
Window thermal OPD	< 0.14 waves rms	0.039 wave rms
Birefringence of input window	<2 nm internal <4 nm thermal and stress	0.6 nm internal 3.1 nm thermal and stress (<111> orientation)

Table 2 - Window Material Selection (1D thermal analysis)

Cell pressure (atm)	55				
Irradiation time (sec)	5				
Pressure aperture radius (cm)	4.36				
Window material	CaF_2	CaF_2	ZBLAN	Al_2O_3	ZnSe
Structure	<100> Cubic	<111> Cubic	Glass	Hexagonal	Cubic
Surface absorption	0.0005	0.0005	0.0005	0.0005	0.0006
Volumetric absorption (1/cm)	0.0002	0.0002	0.0001	0.0002	0.0007
Thermal expansion coeff. (/K)	1.89E-05	1.89E-05	1.68E-05	8.40E-06	7.10E-06
Density (gm/cm3)	3.179	3.179	4.33	3.98	5.27
Index of refraction	1.42	1.42	1.50	1.72	2.44
Index derivative with temperature (/K)	-8.4E-06	-8.4E-06	-1.35E-05	1.30E-05	6.44E-05
Piezo-optic coefficient (/psi)	1.04E-08	1.38E-10	2.00E-10	4.14E-09	1.38E-08
Specific heat (J/gm-K)	0.812	0.812	0.632	0.774	0.339
Thermal conductivity (w/cm-K)	0.097	0.097	0.00628	0.27	0.18
Elastic modulus (psi)	1.49E+07	1.49E+07	7.80E+06	5.00E+07	9.75E+06
Poisson ratio	0.25	0.25	0.31	0.25	0.28
Window thickness (cm)	6.924	6.924	7.132	2.448	8.696
Peak temp. rise from bulk heating (K)	12.28	12.28	5.79	10.29	62.11
Peak temp. rise from surface heating (K)	79.92	79.92	305.08	43.85	84.63
Rms figure OPD (HF wave)	0.00551	0.00551	0.00551	0.00551	0.00551
Rms thermal OPD (HF wave)	9.54E-03	9.54E-03	-1.06E-02	6.73E-02	2.15E+00
Rms total OPD (HFwave)	0.01102	0.01102	0.01193	0.06753	2.14933
Rms thermal birefringence (nm)	1072	14.1	7.6	590	7839
Rms pressure birefringence (nm)	4.3	0.1	0.1	2.8	30
Rms total birefringence (nm)	1072	14.1	7.6	590	7839

Table 3 - Window Stress and Reliability

Load Case	Failure Probability (%)	Maximum Tensile Stress (nt/cm2)
Pressure only	1.59	821.4
Preload only	0.03	129.7
Preload + 55 ATM pressure	1.15	765.0
Preload + 55 ATM pressure + 5 s heating	0.48	918.3

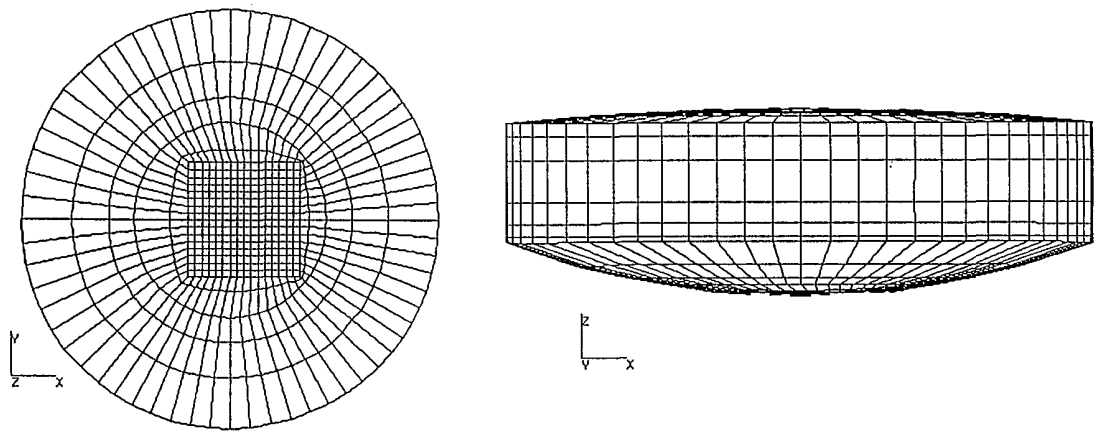

Figure 2 - Finite Element Model

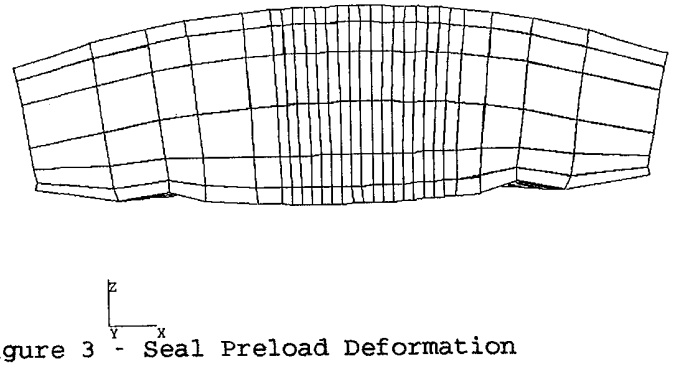

Figure 3 - Seal Preload Deformation

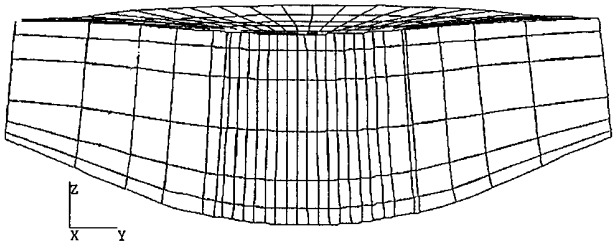

Figure 4 - Pressure Deformation

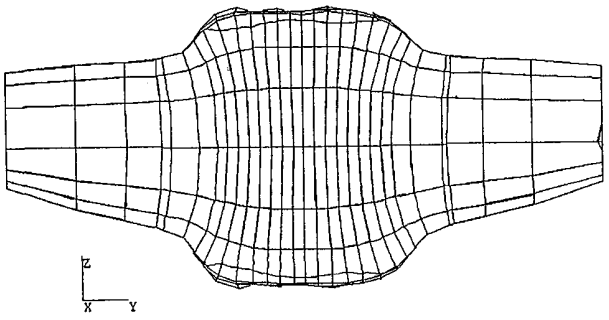

Figure 5 - Beam Heating Deformation

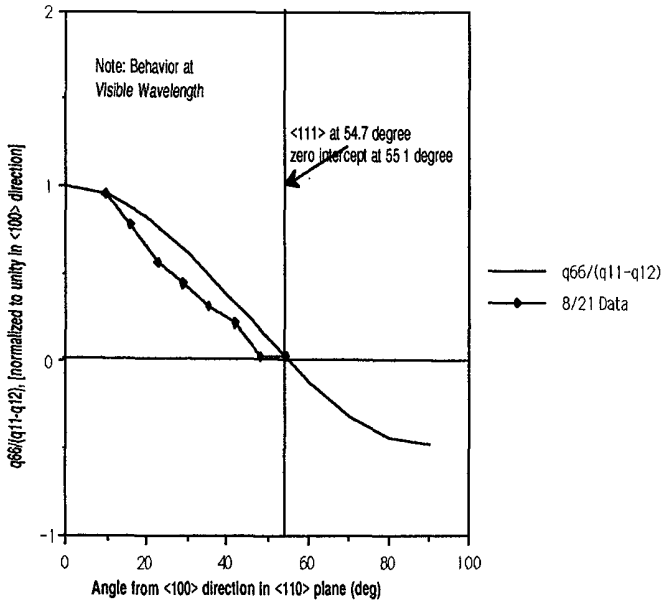

Figure 6 - Sensitivity of CaF2 Piezoptic Coefficient to Crystal Orientation

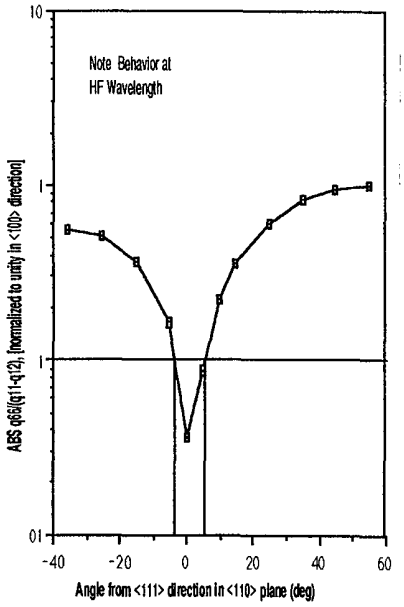

Figure 7 - Alignment Tolerance Required to <111> Direction

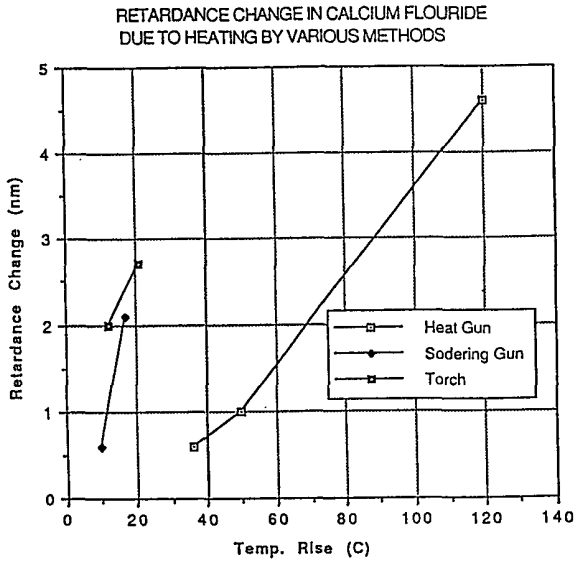

Figure 8 - Thermal Birefringence Tests

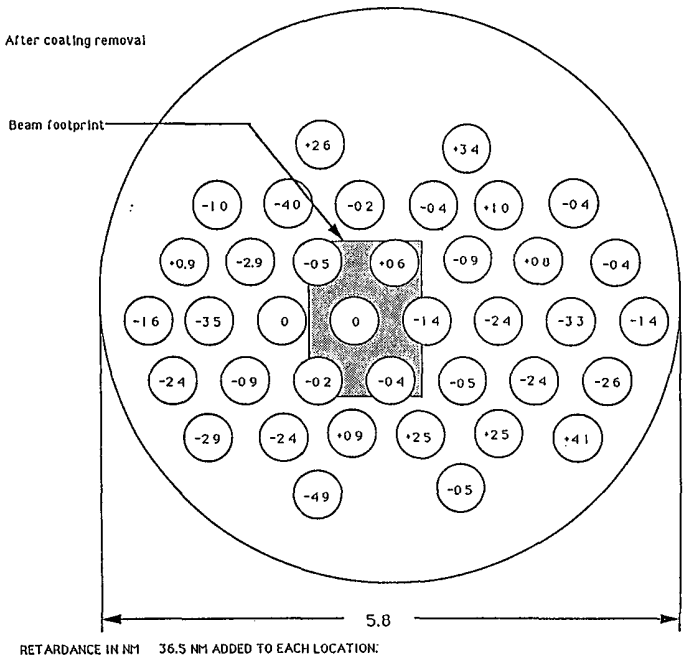

Figure 9 - Internal Stress Birefringence of Input Window Blank